European Review for Medical and Pharmacological Sciences 2019; 23: 5714-5729

Long noncoding RNA DDX11-AS1 induced by YY1 accelerates colorectal cancer progression through targeting miR-873/CLDN7 axis

J.-B. TIAN, L. CAO, G.-L. DONG

Department of General Surgery, the Frist Medical Centre of Chinese of General Hospital, Haidian, Beijing, China

Abstract. – OBJECTIVE: Increasing studies have confirmed long non-coding RNAs (lncRNAs) as novel regulators in tumorigenesis. LncRNA DDX11 antisense RNA 1 (DDX11-AS1) has been found to be abnormally expressed in several tumors. In this work, we aimed to evaluate its expressions and functions in colorectal cancer (CRC).

PATIENTS AND METHODS: The Cancer Genome Atlas (TCGA) datasets were used for the identification of dysregulated lncRNA in CRC. The levels of DDX11-AS1 were determined in tumor tissues and cell lines by Real Time-Polymerase Chain Reaction (RT-PCR). The clinical significance of DDX11-AS1 in CRC patients was analyzed using Chi-square test and Kaplan-Meier analysis. Functional assays for the exploration of DDX11-AS1 and miR-873 were performed using a series of cells experiment. ChIP assay and luciferase reporter assays were used to explore the mechanism of actions of DDX11-AS1 in CRC cells.

RESULTS: We identified DDX11-AS1 as a new CRC-related lncRNA whose levels were distinctly up-regulated in CRC specimens and cell lines, partly induced by YY1. Clinical explorations suggested that increased expressions of DDX11-AS1 in CRC were positively associated with lymph nodes metastasis and TNM stage and had a distinct influence on the overall survival. Further multivariate assays indicated that DDX11-AS1 was an independent prognostic parameter implying a poorer clinical outcome for patients with CRC. Functional assays revealed that the knockdown of DDX11-AS1 suppressed the proliferation, migration, and invasion of CRC cells, and stimulate apoptosis. Mechanistic studies showed that the up-regulation of DDX11-AS1 competitively bound to miR-873 prevented CLDN7 from miRNAs-mediated degradations, thus facilitated the CRC progress. Further rescue assays were carried out to achieve confirmation.

CONCLUSIONS: Our present findings may enhance our understanding of the pathogenesis of CRC and revealed DDX11-AS11 as a potential therapeutic target for CRC.

Key Words:
LncRNA, DDX11-AS11, YY1, MiR-873, CLDN7, Prognosis, Metastasis.

Introduction

Colorectal cancer (CRC), accounting for fifteen percent of all new tumor cases, ranks as the fourth leading cause of cancer death worldwide and is the most common type of gastrointestinal neoplasm[1]. In recent years, due to its special habits and customs, several patients were diagnosed with CRC, leading to it as one of the most prevalent tumors in China[2,3]. The pathogenesis and driving factors of CRC are extremely complex and its accurate mechanism remains largely unclear, but increasing evidence reveal metabolic alternations as important contributors[4]. Although frequent improvements for CRC treatments have been achieved by the use of surgical excision, radiotherapy, and chemotherapy, about 45% of patients exhibit tumor recurrence, which will result in an unfavorable clinical outcome, with a lifetime of only 12.5 months[5,6]. Growing evidence has indicated that tumor metastasis results in recurrences of most CRC[7]. Thus, the identification of novel and effective curative treatment for the improvement of survival rate of CRC patients requires an enhanced discovery of the molecular mechanisms underlying the metastasis of CRC.

Long non-coding RNAs (lncRNAs) are a group of RNAs more than 200 nt in length[8]. Unlike the coding RNA, lncRNAs are found to have limited or no protein-coding capacities, but several reports[9,10] have confirmed them as novel players in the regulation of genes expressions via transcriptional and post-transcriptional modulation. In addition, the involvement of lncRNAs in gene reg-

Corresponding Author: Guang-long Dong, MD; e-mail: tianjingbo1226@126.com

ulations highlights their biological functions in cellular growth, differentiation, immune responses, and several different human developmental pathways[11,12]. Emerging studies[13-15] have provided evidence that lncRNAs may be involved in the progression of various tumors, especially resulting in the dysregulation of tumor-related genes that may serve as contributors in the progression of tumors. Besides, the potential mechanism of lncRNAs displaying its functions is rapidly developing and a newly described regulatory mechanism according to which lncRNAs could inhibit expressions miRNAs via functioning as competitive endogenous RNAs (ceRNAs) becomes the research highlights[16,17]. In recent years, although more and more lncRNAs have been functionally characterized, the mechanism of dysregulation of lncRNAs and their effects involved in the tumor progression remains to be further studied.

LncRNA DDX11 antisense RNA 1 (DDX11-AS1) was originally described by Shi et al[18] who firstly reported DDX11-AS1 was abnormally expressed in hepatocellular carcinoma. It is transcribed from a gene located on chromosome 12p11.21. Up to date, the researches of DDX11-AS1 in the tumor were very limited and its expression and function in CRC have not been determined. In this study, we would like to investigate whether DDX11-AS1 was dysregulated in CRC and further explore its associations with clinical outcome in CRC. Besides, the oncogenic activities of DDX11-AS1 were also examined using *in vitro* assays.

Patients and Methods

Patients Samples

The pathological samples used in this study were collected from 119 CRC patients who underwent surgical resection at the Frist Medical Centre of Chinese of General Hospital between April 2009 and September 2012. The tissue specimens from untreated patients were diagnosed by pathologists before being stored at –80°C. The Ethics Committee of the Frist Medical Centre of Chinese of General Hospital approved the use of the tumor specimens. All the CRC patients signed the written informed consents.

Cell Transfection

Cells were bought from Shanghai Cell Banks (CAS, Xuhui, Shanghai, China), including CRC cells (HCT116, SW480, LOVO, SW116) and FHC cells (control cells). Roswell Park Memorial Institute-1640 (RPMI-1640) media (with 10% serum) were used for cell culture and cells were grown at 37°C with 5% CO_2. Small interfering RNAs (siRNAs) including YY1 siRNA, DDX11-AS1 siRNAs (si-1, si-2), control siRNA (si-NC), miR-873 mimics or inhibitors, control miRNA mimics or inhibitors were purchased from GenePharma company (Suzhou, Jiangsu, China). Besides, YY1, DDX11-AS1, and CLDN7 were respectively cloned into a pcDNA3.1 empty vector (pcDNA3.1-YY1, pcDNA3.1-DDX11-AS1, pcDNA3.1-CLDN7) by Biosee Biological company (Wuhan, Hubei, China). The siRNAs, miRNA mimics or inhibitors, and plasmids were transfected into cells using Lipofectamine 3000 reagents kits (Chengdu, Sichuan, China).

Real Time PCR Reaction

Total RNAs from tissue specimens were extracted using TRIzol reagents (BoJin, Xi'an, Shanxi, China). The RNAs were then quantified by the NanoDrop apparatus. Thereafter, total RNAs were reversely transcripted into cDNAs using the protocols of cDNA synthesis kits (Xiamen, Fujian, China). Then, qPCR reactions for DDX11-AS1 and CLDN7 were conducted using TransGen SYBR Green qPCR kits (Zhengzhou, Henan, China). The qPCR reaction conditions were: 95°C for 5 min; 39 cycles of 95°C for 20 s, 60°C for 1 min; 72°C for 30 s. The results of qPCR were analyzed according to the $2^{-\Delta\Delta Ct}$ methods. Glyceraldehyde 3-phosphate dehydrogenase (GAPDH) was used as the internal reference for DDX11-AS1 and CLDN7. For the miR-873 detection, TransGen two-step miRNA qPCR detection kits were used based on the kits' protocols. U6 was used as the internal control for miR-873. The primers were presented in Table I.

Cell Proliferation Examination

HCT116 cells and SW480 cells were respectively planted into nighty-six well plates (2.5×10^3 cells/well). Subsequently, the determination of cellular proliferation was conducted at 1-4 days. After placing Cell Counting Kit-8 (CCK8) reagents (10 μl/well; Sanyi, Binhai, Tianjin, China) into the cells, the plates were kept in an incubator for 1.5 h. Then, the absorbance at 450 nm was examined using a microplate reader machine.

Clonogenic Assay

CRC cells (600 cells) were plated in six-well plates containing 2 ml media with 10% fetal

Table I. Sequence of the primers used in this study.

Names	Primer sequences (5'-3')
DDX11-AS1: Forward	TCTACCTACCTGTGCGTGGCA
DDX11-AS1: Reverse	CAAGGTAGATCAGGCTACCC
YY1: Forward	ACGGCTTCGAGGATCAGATTC
YY1: Reverse	TGACCAGCGTTTGTTCAATGT
miR-873: Forward	CTGCACTCCCCCACCTG
miR-873: Reverse	GTGCAGGGTCCGAGGT
CLDN7: Forward	AGCTGCAAAATGTACGACTCG
CLDN7: Reverse	GGAGACCACCATTAGGGCTC
U6: Forward	ACACCAAGCAGTCCGAAGAG
U6: Reverse	ACAAAATTTCTCACGCCGGT
GAPDH: Forward	GGAGCGAGATCCCTCCAAAAT
GAPDH: Reverse	GGCTGTTGTCATACTTCTCATGG

bovine serum (FBS) and the plates were placed in an incubator for two to three weeks. The formed cell clones were treated using methanol (25%) and crystal violet (0.1%) for 15 min. After washing, the clones were observed using a microscope.

TUNEL Assay

Cell apoptosis was analyzed by the use of TUNEL detection kits (Fuzhou, Fujian, China). Cells in forty-eight well plates were sequentially treated with paraformaldehyde (4%) and 0.1% Triton X-100. Subsequently, 150 μl (per well) TUNEL reaction buffer was added into the cells. After the cell nuclei were stained using 4',6-diamidino-2-phenylindole (DAPI), the cell fluorescence was observed by a fluorescence microscope.

Flow Cytometry Detection

Cells were plated in six-well plates and grew to 70% confluence, followed by DDX11-AS1 siRNAs transfection. After culturing for 36 h, the cells were digested with trypsin and the single cell suspensions were then prepared. For cell cycle analyses, RNAse propidium iodide (PI) dye reagents and RNase A solution were added into the cell suspensions. For cell apoptosis detection, Annexin-FITC/PI mixture was placed into the cells. After incubation for a period of time, the cells were washed and subjected to flow cytometry analyses. Annexin apoptosis detection kits were bought from BioFeng Biological company (Hefei, Anhui, China).

Wound-Healing Analyses

In short, 4×10^5 cells were plated into six-well plates and allowed to grow to a full confluence. Next, nonadherent cells were removed, followed by being scratched with pipette tips (200 μl) to generate artificial wounds. The wound closures were photographed using a microscope at 0 h and 48 h after the wounds were generated.

Transwell Assay

HCT116 or SW480 cells (2×10^5 cells/well) were collected and counted, followed by being implanted in the top chambers (pre-coated with Matrigel) of the BD Biosciences transwell inserts (pore size: 8 μm; Xiannan, Qingdao, Shandong, China). The media in the top chambers were not allowed to add serum. Media (with 15% serum) were added into the bottom wells as chemical attractants. After incubation for 24 h, cells invaded through the pores were treated using methanol (25%) and crystal violet (0.1%) for 15 min. After washing, the cells were observed using a microscope.

Subcellular Fractionation Assay

Life Technology PARIS kits were employed to separate nuclear and cytoplasmic fractions according to the kits' protocols. Then, qPCR detection was conducted to evaluate the expressing ratios of DDX11-AS1 in cell nuclei or cytoplasm. U6 and GAPDH acted as the nuclear and cytoplasm reference, respectively.

ChIP Assay

Chromatin immunoprecipitation (ChIP) assays were conducted to evaluate the binding between YY1 and DDX11-AS1 promoter regions using CST SimpleChIP kits (Haimen, Jiangsu, China). Cells in 6 cm dishes were cross-linked with formaldehyde (1%) for 10 min. Then, the reactions were quenched by glycine buffer (0.125 M). After washing, the cells were

collected in the ChIP reaction buffer, followed by being sheared to 100 to 500 bp DNA fragments using a sonicator. Then, anti-YY1 antibody (Pudong, Shanghai, China) with IgG as control was applied to precipitate the chromatin. The complexes were incubated with Invitrogen protein G Sepharose (Shenzhen, Guangdong, China) and then eluted from the beads. Finally, qPCR detection was employed to examine the immunoprecipitated chromatin DNAs.

RNA Pull-Down

Biotin-labeled DDX11-AS1 (Biotin-DDX11-AS1) and control lncRNA (Biotin-NC) were bought from Ribo Biological corporation (Guangzhou, Guangdong, China). Then, Biotin-DDX11-AS1 and Biotin-NC were respectively dissolved in RNase-free ultrapure water. Subsequently, Biotin-DDX11-AS1 and Biotin-NC were separately immobilized on the surface of Thermo Fisher Scientific Dynabeads MyOne Streptavidin T1 Beads (JinYouBio, Changsha, Hunan, China). Then, cells were lysed in lysis buffer containing RNase inhibitor. The supernatants were then collected from cell lysates by centrifugation (10,000 × g, 4°C, 10 min). Afterward, Biotin-DDX11-AS1-beads and Biotin-NC-beads were respectively incubated with the supernatants at 4°C for 1.5 h. Finally, the precipitated RNAs were purified and foldchanges of miR-873 was determined by the qPCR detection.

Western Blot

Cells were collected and treated using radioimmunoprecipitation assay (RIPA) reagents (Jinan, Shandong, China). After measuring the protein concentration by bicinchoninic acid (BCA) kits (Chengdu, Sichuan, China), 20 μg (per lane) proteins were separated by 10% sodium dodecyl sulphate-polyacrylamide gel electrophoresis (SDS-PAGE). After the proteins were transferred onto polyvinylidene difluoride (PVDF) membranes, we blocked the membranes with bovine serum albumin (BSA) solution (5%) for 1 h, and then applied CLDN7 antibody (Pudong, Shanghai, China) to probe the membranes. After incubation at 4°C for 12 h, the membranes were washed using Tris-Buffered Saline and Tween-20 (TBST) and incubated with matched secondary antibodies. After rinsing for three times, enhanced chemiluminescence (ECL) assay kits (Jindigene, Dalian, Liaoning, China) was employed for proteins visualization.

Luciferase Activity Detection

The sequence of DDX11-AS1containing wild-type miR-873 binding site was constructed into a pGL3 vector (named as DDX11-AS1 wt). Similarly, the sequence of DDX11-AS1containing mutant-type miR-873 binding site was also cloned into a pGL3 vector (named as DDX11-AS1 mut). Also, to verify the interaction of CLDN7 and miR-873, the luciferase reporter vectors were termed CLDN7 wt and CLDN7 mut, respectively. Furthermore, the sequence containing site#2 (predicted by JASPAR algorithm) was also constructed into pGL3 vector (named as site#2 wt) and corresponding mutant luciferase reporter vector was named as site#2 mut. All the constructs were obtained from Biosee Biological company (Wuhan, Hubei, China). After the cells were treated with corresponding luciferase reporter plasmids with miR-873 mimics, the luciferase activities were carried out following the protocols of Promega Luciferase Reporter Assay kits (Changsha, Hunan, China).

Statistical Analysis

The data was analyzed using SPSS 23.0 software (SPSS, Chicago, IL, USA). The significance of differences was assessed using the Student's *t*-test or a one-way ANOVA. The correlations between DDX11-AS1 expressions and clinical-pathological parameters were determined using chi-square tests. For overall survival curves analyses, we used Kaplan-Meier methods with the log-rank test. Survival data were assessed using univariate and multivariate assays. A value of $p < 0.05$ was considered statistically significant.

Results

Identification of DDX11-AS1, which was Upregulated in CRC Specimens and Cells Lines

To identify novel functional lncRNAs in CRC, we first downloaded CRC TCGA data and subsequently applied bioinformatics analyses to obtain the differentially expressed (DE) lncRNAs. Volcano analyses displayed a clear distinction of lncRNAs between CRC tumor specimens and matched normal samples (Figure 1A). Among these DE-lncRNAs, DDX11-AS1 attracted our attention and we found that DDX11-AS1 was a remarkably high expression in CRC specimens by analyzing TCGA data (Figure 1B). Thereafter, using the "Cancer RNA-seq Nexus" algorithm,

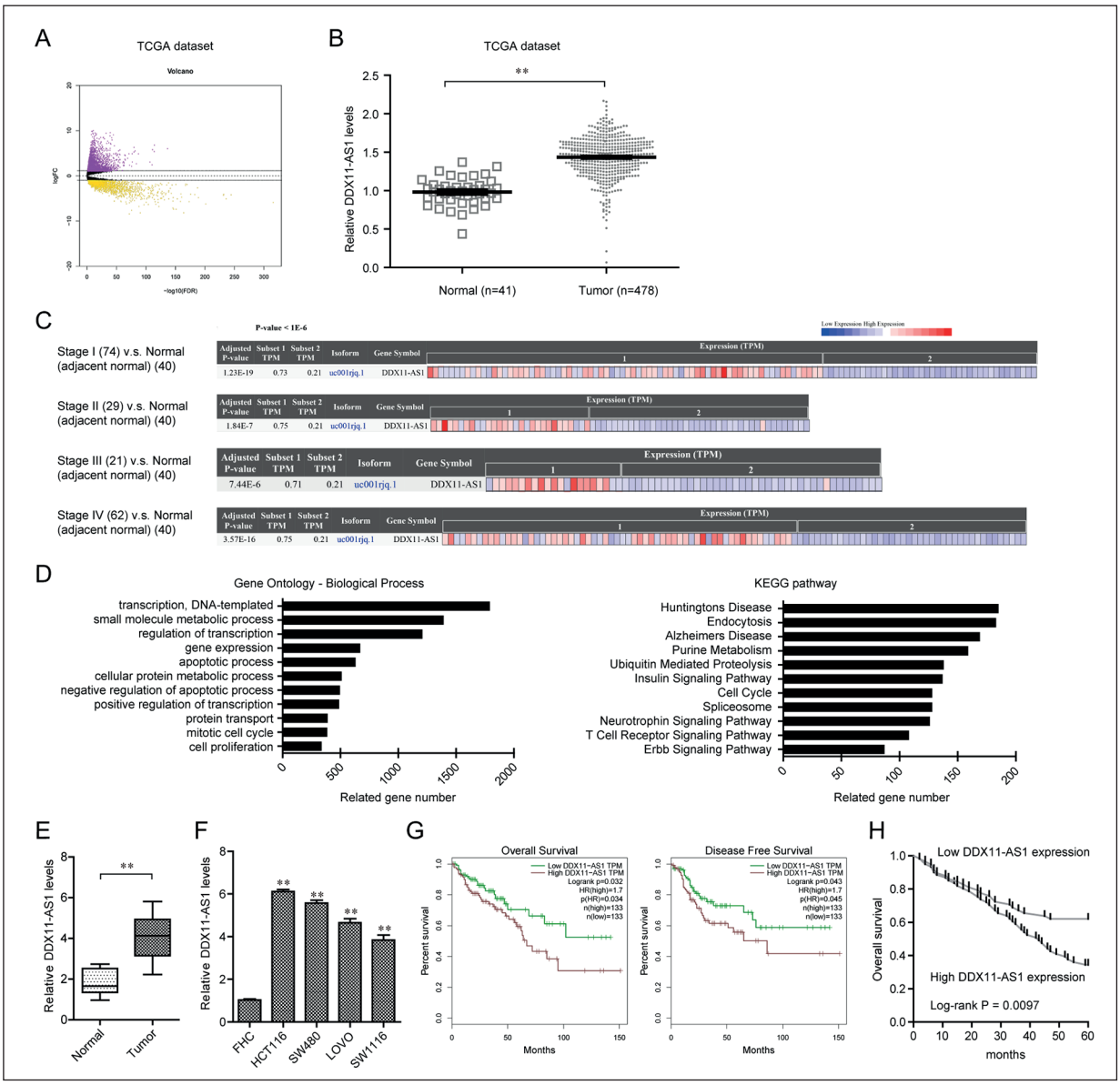

Figure 1. DDX11-AS1 was upregulated in CRC and associated with poor prognosis. **A,** Volcano map of differentially expressed lncRNAs in CRC specimens using TCGA dataset analyses. **B,** DDX11-AS1 was up-regulated in CRC tumor samples using TCGA dataset analyses. **C,** DDX11-AS1 expressing data (from stage I to IV) from TCGA dataset was analyzed by "Cancer RNAseq Nexus" algorithm. **D,** Gene Ontology and KEGG pathway of DDX11-AS1-related genes in CRC were analyzed using "Co-LncRNA" algorithm. **E,** Relative expression of DDX11-AS1 in 119 CRC patients was detected by qPCR assays. **F,** Relative expression of DDX11-AS1 in CRC cells. **G,** "GEPIA" algorithm (using TCGA dataset) analyzed the overall survival and disease-free survival of CRC patients with high or low DDX11-AS1 levels. **H,** Overall survival analyses of 119 CRC patients with high or low DDX11-AS1 expression. * $p < 0.05$, ** $p < 0.01$.

we found that DDX11-AS1 expression was elevated in all stages of CRC samples compared with corresponding normal specimens (Figure 1C). Further Gene Ontology and KEGG pathway analyses using "Co-LncRNA" algorithm indicated that DDX11-AS1 was relevant with transcription, apoptosis, cell cycle, cell proliferation, etc. (Figure 1D). Then, to further demonstrate whether the levels of DDX11-AS1 were dysregulated in CRC, our group performed RT-PCR assays in the CRC tissues and matched normal samples, finding that CRC specimens exhibited higher levels of DDX11-AS1 than normal specimens ($p < 0.01$, Figure 1E). In addition, the data from the analysis

Table II. Association between DDX11-AS1 expressions in tissue specimens from CRC patients and various clinicopathological characteristics.

Parameters	Group	Total	DDX11-AS1 expression		*p*-value
			High	Low	
Gender	Male	63	33	30	0.650
	Female	56	27	29	
Age (years)	< 60	59	26	33	0.169
	≥ 60	60	34	26	
Tumor size (cm)	< 5	76	35	41	0.205
	≥ 5	43	25	18	
Lymph nodes metastasis	Negative	86	37	49	0.009
	Positive	33	23	10	
TNM stage	I-II	77	33	44	0.025
	III-IV	42	27	15	

of DDX11-AS1 expressions in several CRC cell lines revealed that the levels of DDX11-AS1 were distinctly higher in four CRC cells than in FHC cells, corresponding to the result in CRC specimens. Overall, our experiment results, together with the above microarray analysis suggested DDX11-AS1 as a novel CRC-related lncRNA whose levels were distinctly up-regulated in CRC and may contribute to the malignant progress of this disease.

Association Between DDX11-AS1 Expressions and Prognosis in CRC Patients

To investigate the clinical significance of DDX11-AS1 in CRC, using the median expressions of DDX11-AS1 as a cutoff value, we categorized 119 patients suffering from CRC into low (n = 59) and high expression (n = 60) groups. The results of the chi-square test indicated that high expressions of DDX11-AS1 were positively associated with lymph nodes metastasis (p = 0.009) and TNM stage (p = 0.025). However, there were no distinct relations between DDX11-AS1 expressions and other clinicopathological factors of CRC patients (Table II). Then, the survival data were downloaded from TCGA datasets and "GEPIA" which was an online bio information procedure performed for the statistical assays. As shown in Figure 1G, higher levels of DDX11-AS1 predicted a poor overall survival and disease-free survival. Moreover, in our cohort, the results of Kaplan-Meier assays also revealed that breast cancer patients with high DDX11-AS1 levels had a significantly shorter overall survival than patients with low DDX11-AS1 levels (p = 0.0097). Using a multivariate Cox regression analysis, DDX11-AS1 expression (HR=2.984, 95% CI: 1.134-4.237, p = 0.013) was an independent predictor of overall survival, in addition to lymph nodes metastasis and TNM stage (Table III). Overall, our clinical assays, together with the assays results from TCGA datasets, highlighted the clinical potential of DDX11-AS1 used as a novel prognostic biomarker for CRC patients.

Table III. Multivariate survival analysis of overall survival and disease-free survival in 214 osteosarcoma patients.

Variable	Univariate			Multivariate		
	HR	95% CI	*p*-value	HR	95% CI	*p*-value
Gender	1.743	0.743-2.331	0.146	–	–	–
Age	1.455	0.829-2.419	0.129	–	–	–
Tumor size	1.863	0.928-2.421	0.115	–	–	–
Lymph nodes metastasis	3.452	1.362-4.882	0.004	3.019	1.129-4.218	0.011
TNM stage	3.011	1.275-4.021	0.007	2.862	1.129-3.668	0.015
DDX11-AS1 expression	3.425	1.345-4.992	0.003	2.984	1.134-4.237	0.013

DDX11-AS1 Accelerated Cell Growth and Repressed Apoptosis

Considering that high expressing level of DDX11-AS1 was correlated with CRC patients' poor survivals, we further assessed the influences of silencing DDX11-AS1 on CRC cellular processes. In HCT116 and SW480 cells, siRNA-mediated knockdown was carried out for manipulating DDX11-AS1 expression, which was determined by the qPCR analyses. The knockdown efficiency of DDX11-AS1 siRNAs (si-1, si-2) was more than 65% in CRC cells (Figure 2A). Functionally, CCK-8 assays demonstrated that repressing DDX11-AS1 levels markedly weakened CRC cell growth curves (Figure 2B). Furthermore, we wondered whether DDX11-AS1 depletion impacted CRC cells clone formation abilities. Based on the results from clonogenic assays, depression of DDX11-AS1 efficiently suppressed the CRC cell clone number (Figures 2C and D). Thereafter, we employed TUNEL assays to detect whether DDX11-AS1 knockdown influenced cellular apoptosis. The data confirmed that apoptotic cells were notably increased in DDX11-AS1-silenced groups when compared with si-NC-transfected group (Figure 2E). Similar results were also observed by the use of flow cytometry analyses that DDX11-AS1 knockdown promoted cell apoptosis (Figure 2F). The cell cycle distribution was also detected in CRC cells after being treated with DDX11-AS1 siRNAs. The data revealed that the cell cycle progression of DDX11-AS1 siRNAs treated cells was markedly arrested in the G0/G1 phase and the percentages of cells in S phase were notably decreased when compared with the si-NC-transfected cells (Figure 2G). Therefore, the above data indicated that the depression of DDX11-AS1 inhibited CRC tumor growth and accelerated cancer cell apoptosis.

DDX11-AS1 Depletion Impaired the CRC Cell Metastasis

We sought to study whether the reduction of DDX11-AS1 could influence the metastatic capacities of CRC cells. Therefore, we respectively performed wound-healing analyses and transwell assays to assess the impacts of DDX11-AS1 depression on cellular migration and invasion. Transwell assays certified that silencing DDX11-AS1 decreased the invaded CRC cell number compared with the control cells (Figure 3A). Then, wound-healing analyses proved that DDX11-AS1 knockdown resulted in faster wounds closures compared with si-NC-transfected cell group (Figure 3B). Hence, these results validated that DDX11-AS1 modulated the CRC metastasis.

YY1 Activated DDX11-AS1 Expression in CRC Cells

Since the above data validated that DDX11-AS1 was highly expressed in CRC, the molecular mechanisms, which led to upregulation of DDX11-AS1, were necessary to be elucidated. Considering that many reports had indicated that lncRNAs could be stimulated by their upstream transcription factors (TFs), we next predicted the TFs which were able to bind to the promoter of DDX11-AS1 using two classical TF prediction algorithms: JASPAR and PROMO. We intersected the predicted results of these two algorithms and found that there were 8 common TFs (Figure 4A). Among these TFs, YY1, a tumor promoter in many cancer types, ranked first with the highest prediction scores. Hence, we next selected YY1 and sought to investigate whether it was capable to activate the DDX11-AS1 expression. Three predicted YY1 binding sites by JASPAR algorithm were shown in Figure 4B. Besides, YY1 was found to be up-regulated in CRC specimens using TCGA dataset and qPCR analyses (Figures 4C and D). Moreover, YY1 siRNA was able to repress YY1 levels in CRC cells, and pcDNA3.1-YY1 could overexpress YY1 (Figure 4E). We thereby respectively transfected YY1 siRNA or pcDNA3.1-YY1 into CRC cells and then applied qPCR analyses to detect whether DDX11-AS1 expression was changed. As expected, silencing YY1 remarkably elevated the DDX11-AS1 levels, while forced expression of YY1 led to a significant decline of DDX11-AS1 expression, which indicated that DDX11-AS1 expression was negatively correlated with YY1 levels (Figure 4F). For further demonstration of the direct binding between YY1 and DDX11-AS1 promoter region, we conducted ChIP assays in HCT116 and SW480 cells. Site#2 fragment, but not site#1 and site#3, was responsible for the affinity of YY1 to DDX11-AS1 promoter (Figure 4G). Besides, luciferase reporter analyses clarified that site#2 wild-type (wt), but not site#2 mutant type, of DDX11-AS1 promoter region driven the luciferase activity (Figure 4H). All the data demonstrated that YY1 transcriptionally activated DDX11-AS1 up-regulation in CRC cells.

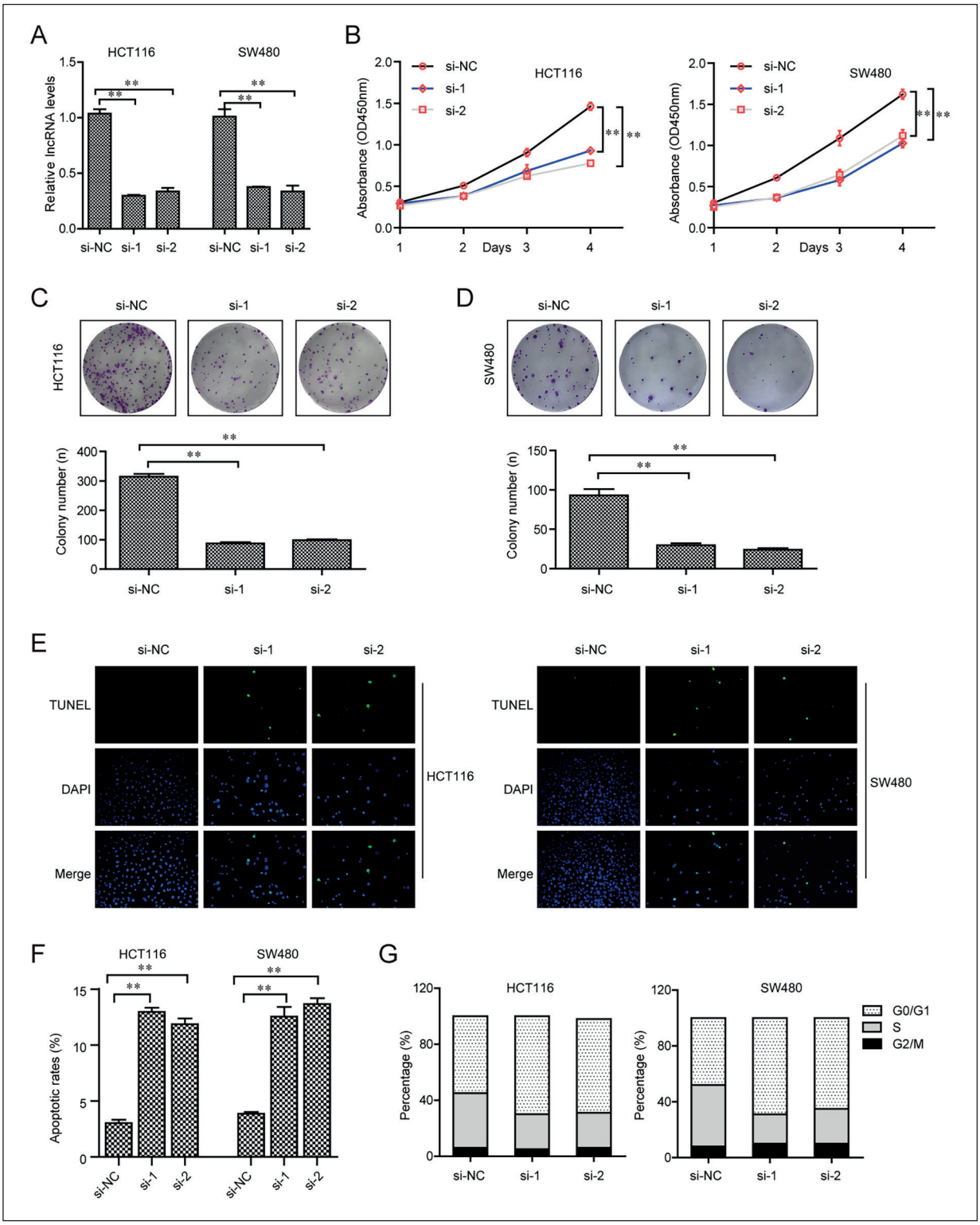

Figure 2. The influences of DDX11-AS1 on cellular growth, apoptosis and cell cycle of CRC cells. **A,** After silencing DDX11-AS1 in CRC cells, interference efficiency of si-1 and si-2 was verified via qPCR. **B,** After knockdown of DDX11-AS1, CCK8 assays were applied to examine the cellular proliferation. **C, D,** Clonogenic assays revealed the impacts of DDX11-AS1 knockdown on CRC cell clone formation capacities (Magnification: 10×). **E,** TUNEL assays detected the cell apoptosis. Green represented apoptotic cells and nuclei were stained by DAPI (blue) (magnification: 100×). **F,** Apoptotic rates of cells were analyzed via flow cytometry. **G,** Cell cycle was analyzed via flow cytometry. * $p < 0.05$, ** $p < 0.01$.

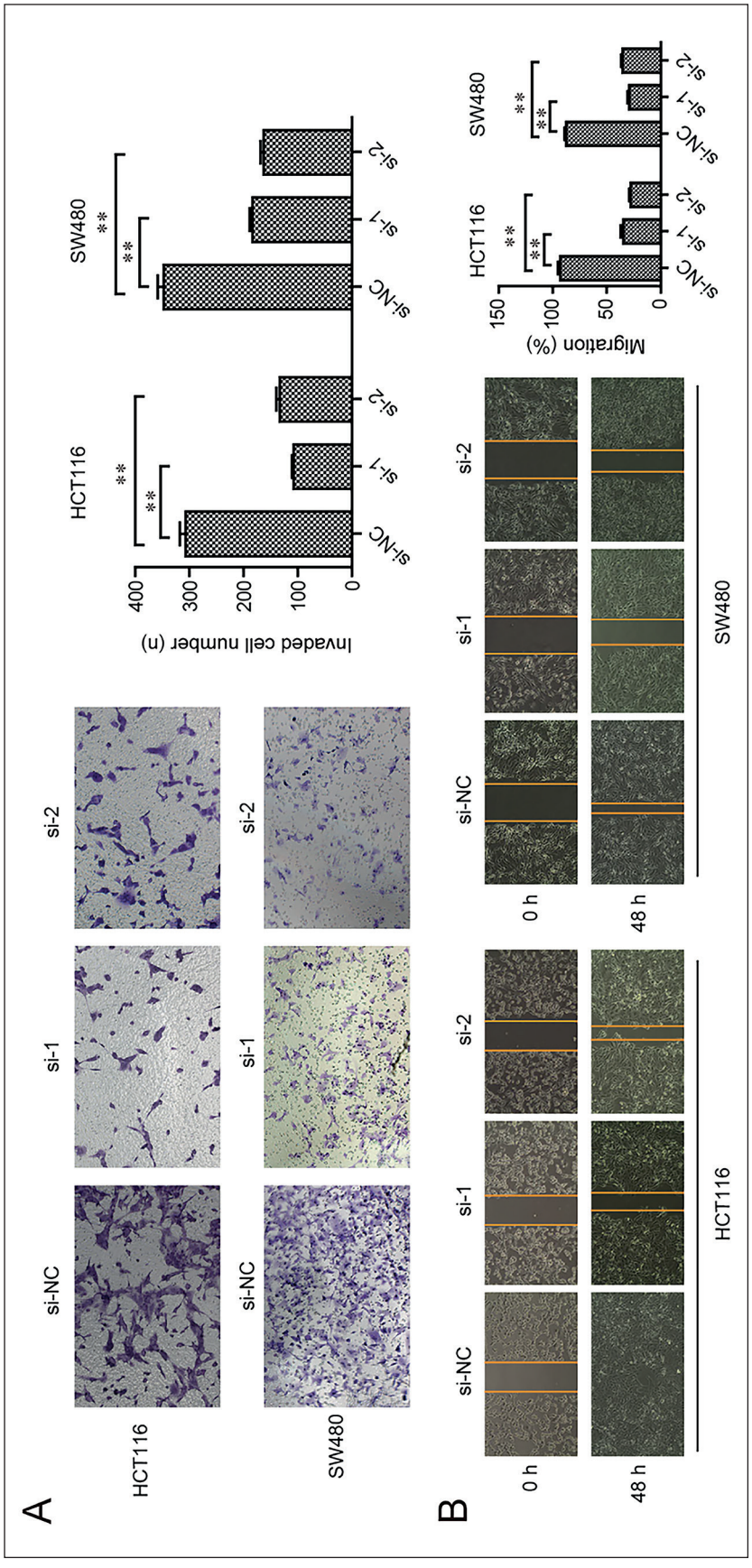

Figure 3. The effects of DDX11-AS1 on CRC cell aggressiveness. **A,** Transwell assays showed that transfection of si-1 and si-2 inhibited CRC cell invasive abilities (Magnification: 40×). **B,** Wound-healing assays presented that depletion of DDX11-AS1 suppressed migration abilities of CRC cells (Magnification: 10×). * $p < 0.05$, ** $p < 0.01$.

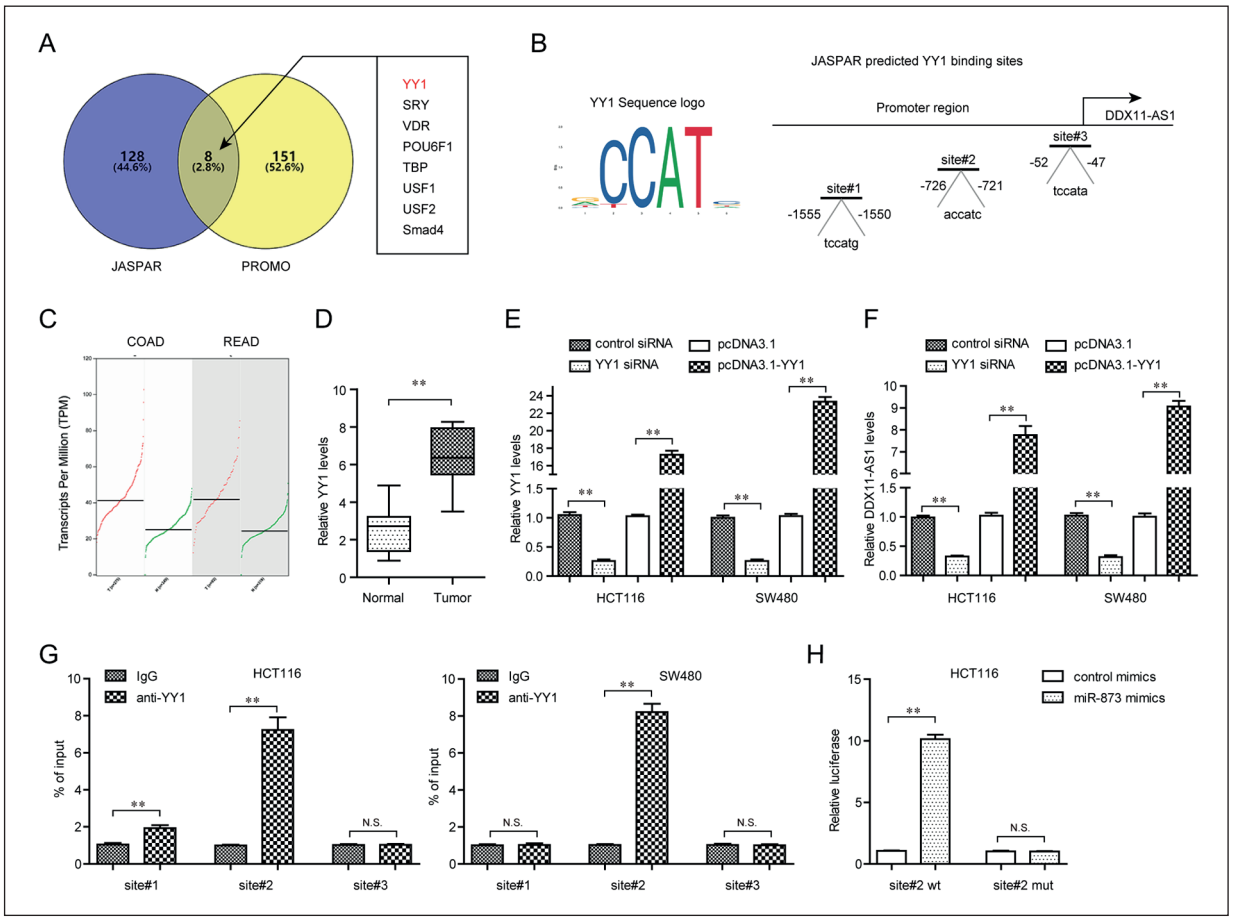

Figure 4. YY1 stimulated DDX11-AS1 expression by acting as a transcription activator. **A,** Intersection between "JASPAR" algorithm predicted results and "PROMO" predicted results. **B,** DNA motif of YY1 and three predicted binding sites (by "JASPAR" algorithm) of YY1 in DDX11-AS1 promoter. **C,** "GEPIA" algorithm analyzed the expressing levels of DDX11-AS1 CRC tumor tissues using TCGA dataset. COAD: Colon adenocarcinoma; READ: Rectum adenocarcinoma. **D,** Relative YY1 levels in 119 CRC patients' samples were detected by qPCR. **E,** QPCR examined the levels of YY1 in CRC cells after being treated with YY1 siRNAs or pcDNA3.1-YY1. **F,** QPCR examined the levels of DDX11-AS1 in CRC cells after YY1 was silenced or overexpressed. **G,** ChIP assays were carried out to detect the affinity of YY1 to DDX11-AS1 promoter. **H,** Luciferase activity detection. * $p < 0.05$, ** $p < 0.01$.

Verification of MiR-873 as a Direct Target of DDX11-AS1 in CRC Cells

To uncover the potential mechanisms underlying DDX11-AS1 participating in regulating CRC tumorigenesis, we first conducted subcellular fractionation assays to determine the subcellular location of DDX11-AS1 since DDX11-AS1 might exert different functions depending on its subcellular location. According to the data, DDX11-AS1 was notably exhibited in the cytoplasm (Figure 5A). Therefore, DDX11-AS1 might sponge potential miRNAs to exert its functions. Using the "starbase" algorithm, we predicted the possible target miRNAs of DDX11-AS1, and we found that miR-873, a tumor suppressor, was a potential target (Figure 5B). Indeed, the KEGG pathway analysis using "starbase" algorithm indicated that the predicted target genes of miR-873 were significantly associated with diverse cancer types and pathway in cancer (Figure 5C). Hence, we next sought to validate miR-873 was the direct target of DDX11-AS1 in CRC cells. To prove this, luciferase reporter assays were first conducted. The data clarified that the luciferase activity in the miR-873 mimics and DDX11-AS1 wild-type (wt) reporter vectors co-transfected-group was remarkably decreased, while co-transfection with miR-873 mimics and DDX11-AS1 mutant-type (mut) reporter vectors did not change the luciferase

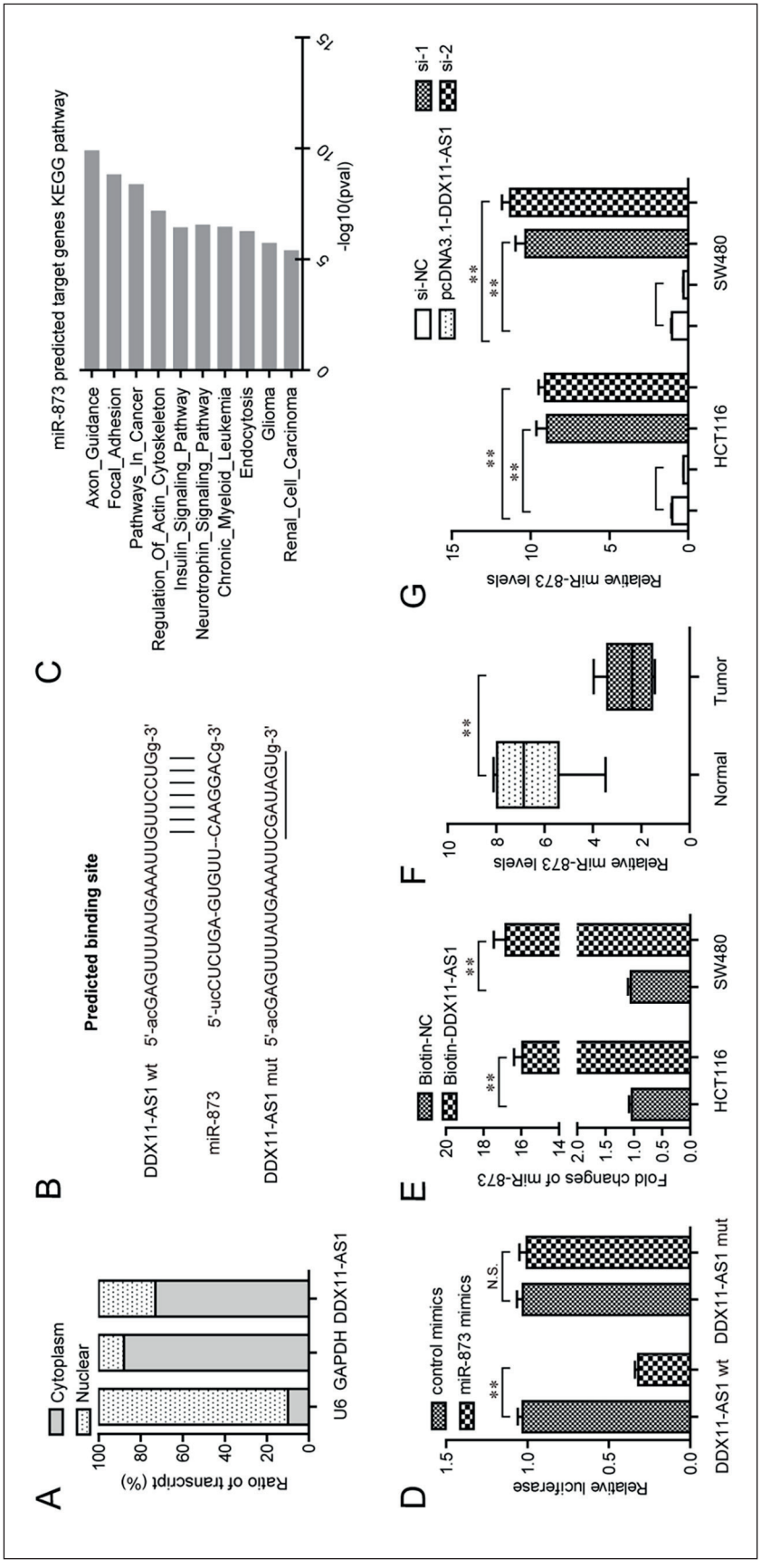

Figure 5. DDX11-AS1 directly interacted with miR-873 in CRC cells. **A,** Subcellular fractionation assays detected the subcellular location of DDX11-AS1 in HCT116 cells. **B,** "Starbase" predicted miR-873 had a binding site on the DDX11-AS1 transcript. **C,** "Starbase" analyzed the KEGG pathway of predicted miR-873 target genes. **D,** Luciferase activity examination assays. **E,** RNA pull-down assays. **F,** Relative miR-873 levels in 119 CRC patients' tumor specimens were measured by qPCR. **G,** Real Time PCR determined the relative miR-873 levels in CRC cells after DDX11-AS1 was silenced or overexpressed. * $p < 0.05$, ** $p < 0.01$.

activities (Figure 5D). Further RNA pull-down analyses manifested miR-873 was remarkably enriched in biotin labeled DDX11-AS1-group compared with NC group (Figure 5E). Therefore, luciferase reporter assays and RNA pull-down analyses confirmed that DDX11-AS1 has directly interacted with miR-873. In addition, qPCR analyses revealed that miR-873 was markedly down-regulated in CRC specimens (Figure 5F). Besides, enhancing DDX11-AS1 expression markedly impeded miR-873 levels in CRC cells, while silencing the levels of DDX11-AS1 notably promoted the miR-873 expressing levels (Figure 5G). All these data proved that miR-873 was a direct target of DDX11-AS1 in CRC cells.

CLDN7 was a Direct Target of MiR-873 in CRC Cells

Increasing evidence[19] has revealed that miRNAs could directly interact with the 3'-UTR of genes and thereby modulate their expressions. Hence, we next sought to discover the target genes of miR-873 to better understand the functions of DDX11-AS1 exerted in CRC cells. We first intersected the predicted target genes of "miRDB", "starbase", and 1000 most highly expressed genes in CRC using TCGA dataset by "GEPIA" analyses, and there were 17 common genes, including CLDN7, an oncogenic promoter in many cancer types (Figure 6A). Indeed, bioinformatics analyses using TCGA dataset demonstrated that CLDN7 was up-regulated in CRC samples (Figure 6B). Subsequently, the qPCR detection also demonstrated that CRC specimens displayed significantly higher CLDN7 levels than that of matched normal tissue samples (Figure 6C). Therefore, we next aimed to prove CLDN7 was a direct target of miR-873. The predicted binding site between miR-873 and 3'-UTR of CLDN7 was shown in Figure 6D. Then, wild-type 3'-UTR of CLDN7 (CLDN7 wt) or mutant-type 3'-UTR of CLDN7 (CLDN7 mut) sequence was respectively constructed into pGL3 luciferase reporter vector, and subsequently, the luciferase reporter assays were conducted. Results suggested that CLDN7 wt was able to reduce the luciferase activities

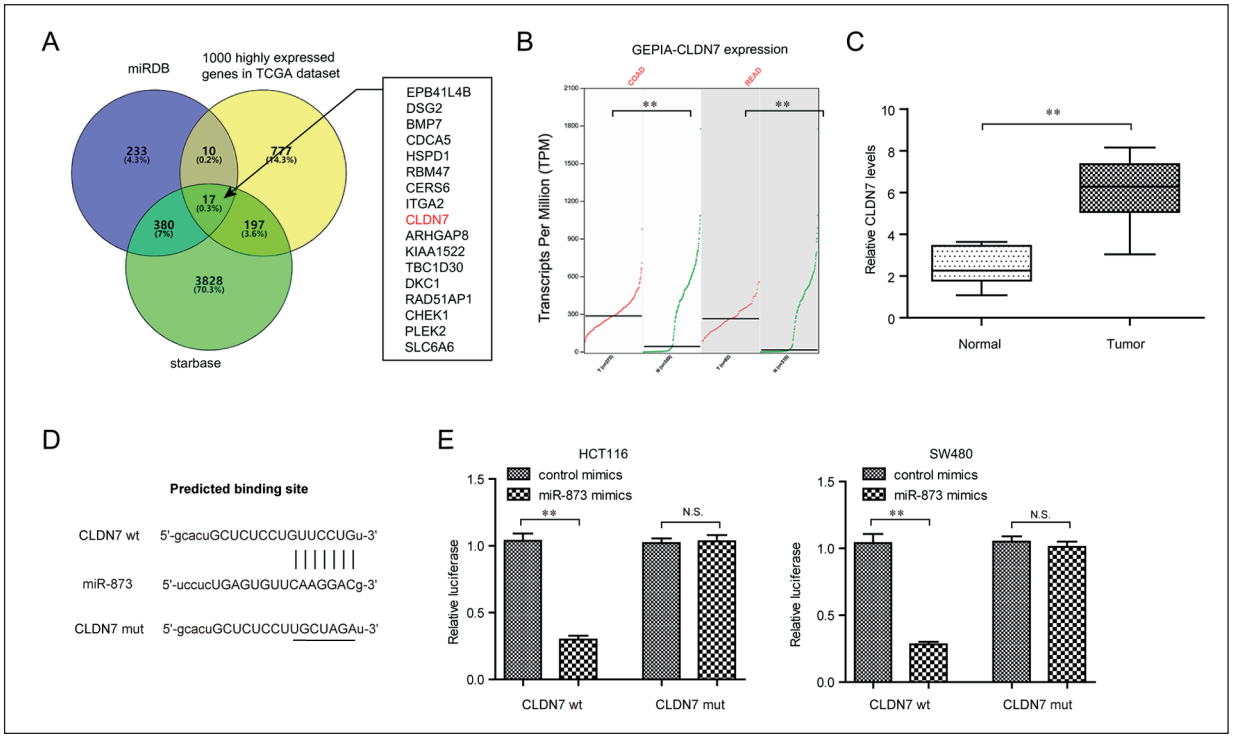

Figure 6. CLDN7 was a target of miR-873 in CRC cells. **A,** Intersection of "miRDB" algorithm predicted results, "starbase" algorithm predicted results and 1000 highly expressed genes in CRC tumor tissues analyzed by "GEPIA" algorithm using TCGA dataset. **B,** CLDN7 levels were up-regulated in CRC tumor specimens using "GEPIA" algorithm analysis. The data was from TCGA dataset. COAD: Colon adenocarcinoma; READ: Rectum adenocarcinoma. **C,** Relative CLDN7 levels in 119 CRC patients' tumor specimens were measured by qPCR. **D,** Binding site between 3'UTR of CLDN7 and miR-873 was predicted by "starbase" algorithm. **E,** Luciferase activity examination assays. * $p < 0.05$, ** $p < 0.01$.

in CRC cells transfected with miR-873 mimics, while co-transfection with CLDN7 mut and miR-873 mimics had no influence on the luciferase activities (Figure 6E). Taken together, these data validated that CLDN7 acted as a direct target of miR-873 in CRC cells.

DDX11-AS1 Exerted its Functions via MiR-873/CLDN7 Axis in CRC Cells

We sought to investigate the relation between DDX11-AS1, miR-873, and CLDN7 in functional regulation. First, we carried out qPCR detection to evaluate the levels of DDX11-AS1 and CLDN7 in CRC cells after their miR-873 was enhanced and silenced. According to the data, both DDX11-AS1 and CLDN7 in cells were suppressed by the miR-873 up-regulation, while levels of DDX11-AS1 and CLDN7 were remarkably promoted by the down-regulation of miR-873, which indicated that miR-873 expressing level was negatively correlated with both DDX11-AS1 and CLDN7 expression in CRC cells (Figure 7A). Subsequently, we examined DDX11-AS1 levels in HCT116 cells after miR-873 or CLDN7 up-regulation. The data from qPCR showed that DDX11-AS1 levels were markedly elevated by CLDN7 overexpression and inhibited by miR-873 up-regulation, while re-introduction of CLDN7 was able to abrogate the suppressing impaction of miR-873 on DDX11-AS1 levels (Figure 7B). These data indicated that DDX11-AS1 expression was negative with miR-873 expression and positive with CLDN7 expression in CRC cells. Afterward, we conducted Western blot analyses to detect CLDN7 protein changes in HCT116 cells after altering DDX11-AS1 or miR-873 expressing levels. Results displayed that transfection with pcDNA3.1-DDX11-AS1 could significantly increase the levels of CLDN7 and miR-873 mimics were capable to markedly depress CLDN7 levels, while re-expressing DDX11-AS1 could significantly restore CLDN7 levels (Figure 7C). Additionally, we next carried out CCK-8 analyses to assess the changes in CRC cell growth curves after the cells were transfected with miR-873 mimics or pcDNA3.1-DDX11-AS1. The results indicated that up-regulation of miR-873 notably depressed the cell growth, while re-transfecting with pcDNA3.1-DDX11-AS1 could notably reverse the cell proliferative rates (Figure 7D). Correspondingly, we observed similar results according to the data of wound-healing analyses that the decreased CRC cell migratory rates by miR-873 up-regulation could be restored by overexpressing DDX11-AS1 (Figure 7E). Overall, these data validated that DDX11-AS1 exerted its functions via miR-873/CLDN7 axis in CRC cells.

Discussion

The morbidity and mortality of CRC are increasing quickly, while effective cancer therapies remain ambiguous in several CRC patients. Early detection and individualized treatments are imperative for long-term overall survival. Identification of sensitive biomarkers is of great importance for the management of patients and a valuable marker must impact clinical judgment making in a manner that resulted in better patients cares[20]. In recent years, several studies[21,22] highlighted the potential of lncRNAs serving as novel biomarkers of CRC patients for diagnosis and prognosis. In this work, we first identified a novel CRC-related lncRNA DDX11-AS1 whose levels in CRC tissues and cell lines were markedly increased by the assays of microarray data and the experiments of RT-PCR. Then, in our clinical investigations, it was observed that higher expressions of DDX11-AS1 were correlated with lymph nodes metastasis, TNM stage, and unfavorable clinical survival. Further multivariate assays confirmed that DDX11-AS1 expression is an independent prognostic factor of overall survival in CRC patients. Our findings revealed DDX11-AS1 as a novel marker which could help the optimization of clinical treatments.

In our present report, we have provided reliable evidence that DDX11-AS1 was highly expressed in CRC. However, the potential mechanism involved in the overexpression of DDX11-AS1 remains unknown. Previously, several studies confirmed the positive associations between dysregulation of DDX11-AS1 and the activation of transcription factors[23]. Of note, several important transcription factors such as SP1 and STAT1 have been frequently reported to be involved in the modulation of numerous lncRNAs in various tumors[24,25]. Yin Yang-1 (YY1), encoded by 23 kb YY1, is ubiquitously expressed zinc finger transcription factor and many functional studies have indicated its involvement in the progression of a variety of cellular processes[26,27]. Notably, the tumor-promotive roles of lncRNAs in cellular growth and metastasis have been confirmed in various tumor and the potential mechanisms are involved in the regulation of tumor-related genes, such as P53. However,

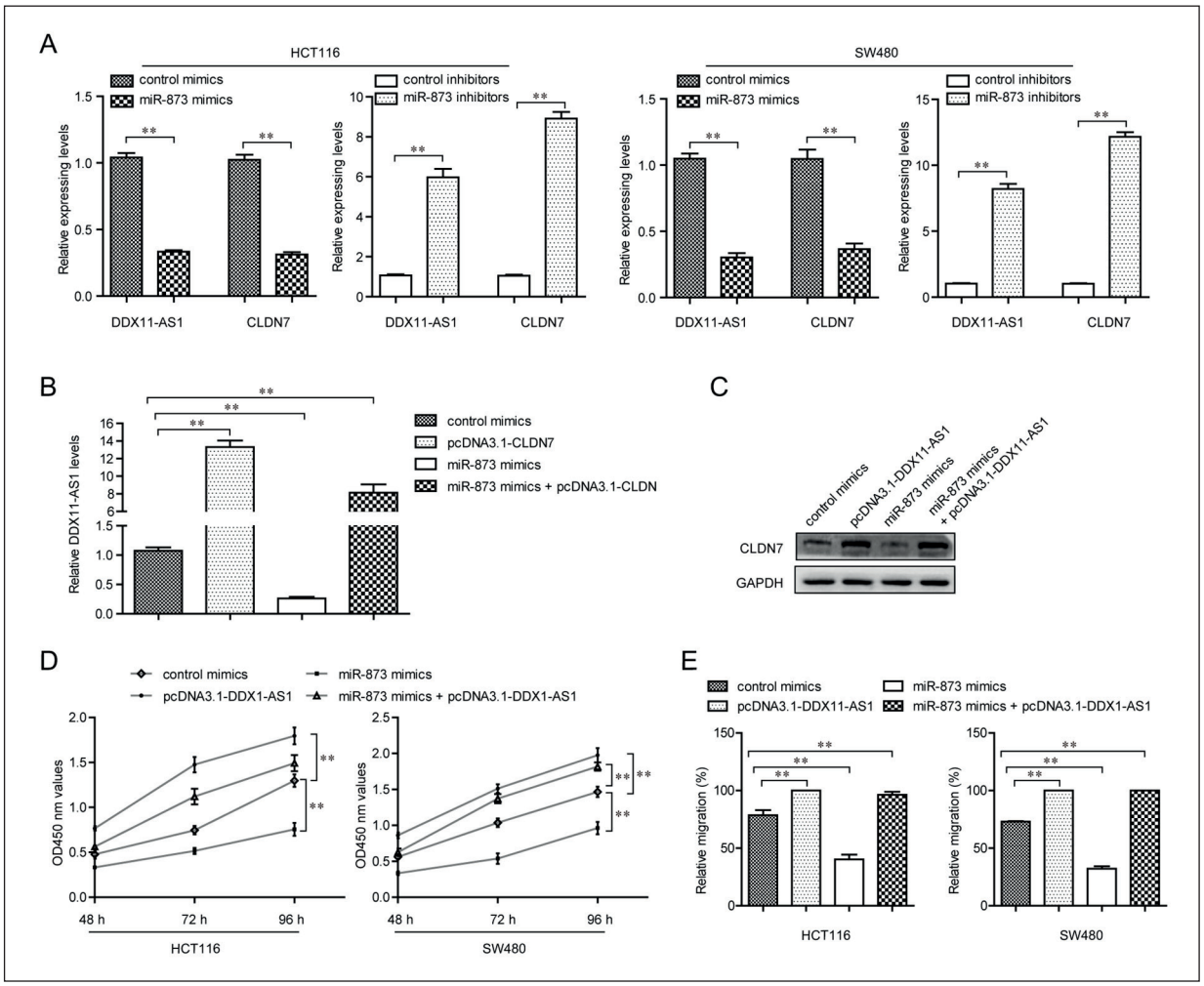

Figure 7. Regulatory relationships among DDX11-AS1, CLDN7, and miR-873 in CRC cells. **A,** Real Time PCR evaluated the levels of DDX11-AS1 and CLDN7 in CRC cells after treatment with miR-873 mimics or inhibitors. **B,** QPCR analyses detected the DDX11-AS1 expression in HCT116 cells after changing the expressions of miR-873 or CLDN7. **C,** Western blot detected the CLDN7 protein levels in HCT116 cells after changing the expressions of miR-873 or DDX11-AS1. **D,** CCK-8 assays assessed the growth curves of CRC cells under various conditions. **E,** Wound-healing assays detected the migratory ability changes of CRC cells after diverse treatment. * $p < 0.05$, ** $p < 0.01$.

whether YY1 can regulate the expressions of lncRNAs remains largely unclear. In this research, by the use of Jaspar and PROMO database, the possible transcription factors which may modulate DDX11-AS1 were screened and YY1 became a positive one due to its higher scores. Furthermore, the results of ChIP and luciferase reporter assays confirmed that YY1 could interact with the promoter of DDX11-AS1, indicating that YY1 may act as a contributor for the activation of DDX11-AS1 translation to further promote the expressions of DDX11-AS1 in CRC.

Previously, the overexpression of DDX11-AS1 has been reported in several tumors, such as hepatocellular carcinoma, gastric cancer, and glioma, indicating its oncogenic roles in these tumors[28-30]. In addition, several clinical and basic experiments also revealed the positive influence of DDX11-AS1 on the cellular and clinical progress of the above tumors. Then, our group performed loss-of-function assays for the study of DDX11-AS1 function in CRC cells and the results revealed that the knockdown of DDX11-AS1 could suppress proliferation, migration, and invasion of CRC cells, as well as promote apoptosis. Our results suggested that DDX11-AS1 functioned as a tumor promoter in CRC.

Growing studies[31] have shown that lncRNAs and miRNAs could interact with each other to develop regulatory networks for the presentation

of their regulatory roles in tumor progression. For instance, lncRNA TUNAR, a down-regulated lncRNA in glioma, was reported to act as a tumor suppressor since its overexpression suppressed the proliferation and metastasis of CRC Cells via modulating miR-200a[32]. Ln-cRNA CCAT2, a well-studied tumor-related ln-cRNA in various tumors, was shown to be highly expressed in lung adenocarcinoma and its knockdown cells proliferation and migration by targeting sponging miR-23b-5p[33]. To investigate the underlying mechanisms of DDX11-AS1-induced proliferation and metastasis suppression, we speculated that DDX11-AS1 may exhibit its roles by modulating miRNAs. Using a series of experiments, our results indicated that DDX11-AS1 acted as an endogenous sponge via binding to miR-873 and, consequently suppressing the levels of miR-873. Previously, miR-873 has been reported to act as a tumor suppressor in various tumors, including CRC[34,35]. Taken together, our findings suggested the cancer-promotive roles of DDX11-AS1 in CRC by sponging miR-873.

To explore whether DDX11-AS1-induced miR-873 suppression leads to a promotion of its mRNA targets and, subsequently stimulating the tumor progress of CRC, we used TargetScan 6.2 for the prediction of potential targeting genes of miR-873, finding that CLDN7 may be a candidate. Previously, many studies[36,37] have confirmed that there is a distinct upregulation of CLDN7 in several tumors, including CRC. Of note, there is a study showing that CLDN7 overexpression contributed to the progress of EMT, indicating its oncogenic regulator in CRC. Using luciferase activity assays, we confirmed that miR-873 can directly target CLDN7 in CRC cells. Then, we explored the association between DDX11-AS1 and miR-873 and CLDN7 in CRC. We found that the overexpression of miR-873 suppressed the levels of DDX11-AS1 and CLDN7, while the up-regulation of miR-873 displayed opposite results. Besides, rescue experiments revealed that the overexpression of CLDN7 rescued the suppressing roles of miR-873 overexpression in regulating the expressions of DDX11-AS1. Moreover, functional assays using rescue model indicated that miR-873 overexpression and CLDN7 down-regulation reversed the regulatory effects of increased DDX11-AS1 on proliferation, migration, and invasion of CRC cells. Overall, our results revealed that DDX11-AS1 contributes to CRC progression via sponging miR-873 to increase CLDN7. Except for DDX11-AS1, other lncRNAs or mRNAs could also be targets of miR-873; however, this requires further investigations.

Conclusions

We revealed that increased DDX11-AS1 expression is a common event and a novel prognostic biomarker in CRC. Furthermore, DDX11-AS1 was activated by YY1 and positively regulated CRC progression via the miR-873/ CLDN7 axis. Taken together, the dysfunctions of the DDX11-AS11/miR-873/CLDN7 axis may be a novel mechanism responsible for CRC.

Conflict of Interest

The Authors declare that they have no conflict of interests.

References

1) Siegel RL, Miller KD, Jemal A. Cancer statistics, 2016. CA Cancer J Clin 2016; 66: 7-30.
2) Chen W, Zheng R, Baade PD, Zhang S, Zeng H, Bray F, Jemal A, Yu XQ, He J. Cancer statistics in China, 2015. CA Cancer J Clin 2016; 66: 115-132.
3) Zhu J, Tan Z, Hollis-Hansen K, Zhang Y, Yu C, Li Y. Epidemiological trends in colorectal cancer in China: an ecological study. Dig Dis Sci 2017; 62: 235-243.
4) Weinberg BA, Marshall JL, Salem ME. The growing challenge of young adults with colorectal cancer. Oncology (Williston Park) 2017; 31: 381-389.
5) Simon K. Colorectal cancer development and advances in screening. Clin Interv Aging 2016; 11: 967-976.
6) Otani K, Ishihara S, Hata K, Murono K, Sasaki K, Yasuda K, Nishikawa T, Tanaka T, Kiyomatsu T, Kawai K, Nozawa H, Yamaguchi H, Watanabe T. Colorectal cancer with venous tumor thrombosis. Asian J Surg 2018; 41: 197-202.
7) Chakedis J, Squires MH, Beal EW, Hughes T, Lewis H, Paredes A, Al-Mansour M, Sun S, Cloyd JM, Pawlik TM. Update on current problems in colorectal liver metastasis. Curr Probl Surg 2017; 54: 554-602.
8) Jathar S, Kumar V, Srivastava J, Tripathi V. Technological developments in lncRNA biology. Adv Exp Med Biol 2017; 1008: 283-323.
9) Jarroux J, Morillon A, Pinskaya M. History, discovery, and classification of lncRNAs. Adv Exp Med Biol 2017; 1008: 1-46.
10) Ferre F, Colantoni A, Helmer-Citterich M. Revealing protein-lncRNA interaction. Brief Bioinform 2016; 17: 106-116.

11) Jandura A, Krause HM. The new RNA world: growing evidence for long noncoding RNA functionality. Trends Genet 2017; 33: 665-676.

12) Li X, Wu Z, Fu X, Han W. LncRNAs: insights into their function and mechanics in underlying disorders. Mutat Res Rev Mutat Res 2014; 762: 1-21.

13) Forrest ME, Khalil AM. Review: regulation of the cancer epigenome by long non-coding RNAs. Cancer Lett 2017; 407: 106-112.

14) Zhao Y, Qin ZS, Feng Y, Tang XJ, Zhang T, Yang L. Long non-coding RNA (lncRNA) small nucleolar RNA host gene 1 (SNHG1) promote cell proliferation in colorectal cancer by affecting P53. Eur Rev Med Pharmacol Sci 2018; 22: 976-984.

15) Zhou FR, Pan ZP, Shen F, Huang LQ, Cui JH, Cai K, Guo XL. Long noncoding RNA DLX6-AS1 functions as a competing endogenous RNA for miR-577 to promote malignant development of colorectal cancer. Eur Rev Med Pharmacol Sci 2019; 23: 3742-3748.

16) Karreth FA, Pandolfi PP. CeRNA cross-talk in cancer: when ce-bling rivalries go awry. Cancer Discov 2013; 3: 1113-1121.

17) Li G, Wang C, Wang Y, Xu B, Zhang W. LINC00312 represses proliferation and metastasis of colorectal cancer cells by regulation of miR-21. J Cell Mol Med 2018; 22: 5565-5572.

18) Shi M, Zhang XY, Yu H, Xiang SH, Xu L, Wei J, Wu Q, Jia R, Wang YG, Lu XJ. DDX11-AS1 as potential therapy targets for human hepatocellular carcinoma. Oncotarget 2017; 8: 44195-44202.

19) Vishnoi A, Rani S. MiRNA biogenesis and regulation of diseases: an overview. Methods Mol Biol 2017; 1509: 1-10.

20) Schirripa M, Lenz HJ. Biomarker in colorectal cancer. Cancer J 2016; 22: 156-164.

21) Okugawa Y, Grady WM, Goel A. Epigenetic alterations in colorectal cancer: emerging biomarkers. Gastroenterology 2015; 149: 1204-1225.

22) Zhou JF, Wang HG, Ma TH, Yan W, Wu SN, Shi YT, Yang XZ. Long noncoding RNA LINC01510 is highly expressed in colorectal cancer and predicts favorable prognosis. Eur Rev Med Pharmacol Sci 2018; 22: 7710-7715.

23) Bunch H. Gene regulation of mammalian long non-coding RNA. Mol Genet Genomics 2018; 293: 1-15.

24) Sheng L, Wu J, Gong X, Dong D, Sun X. SP1-induced upregulation of lncRNA PANDAR predicts adverse phenotypes in retinoblastoma and regulates cell growth and apoptosis in vitro and in vivo. Gene 2018; 668: 140-145.

25) Shen Y, Gao X, Tan W, Xu T. STAT1-mediated upregulation of lncRNA LINC00174 functions a ceRNA for miR-1910-3p to facilitate colorectal carcinoma progression through regulation of TAZ. Gene 2018; 666: 64-71.

26) Khachigian LM. The Yin and Yang of YY1 in tumor growth and suppression. Int J Cancer 2018; 143: 460-465.

27) Pothoulakis C, Torre-Rojas M, Duran-Padilla MA, Gevorkian J, Zoras O, Chrysos E, Chalkiadakis G, Baritaki S. CRHR2/Ucn2 signaling is a novel regulator of miR-7/YY1/Fas circuitry contributing to reversal of colorectal cancer cell resistance to Fas-mediated apoptosis. Int J Cancer 2018; 142: 334-346.

28) Liao HT, Huang JW, Lan T, Wang JJ, Zhu B, Yuan KF, Zeng Y. Identification of the aberrantly expressed lncRNAs in hepatocellular carcinoma: a bioinformatics analysis based on RNA-sequencing. Sci Rep 2018; 8: 5395.

29) Liu H, Zhang Z, Wu N, Guo H, Zhang H, Fan D, Nie Y, Liu Y. Integrative analysis of dysregulated lncRNA-associated ceRNA network reveals functional lncRNAs in gastric cancer. Genes (Basel) 2018; 9. pii: E303

30) Luan F, Chen W, Chen M, Yan J, Chen H, Yu H, Liu T, Mo L. An autophagy-related long non-coding RNA signature for glioma. FEBS Open Bio 2019; 9: 653-667.

31) Giza DE, Vasilescu C, Calin GA. MicroRNAs and ceRNAs: therapeutic implications of RNA networks. Expert Opin Biol Ther 2014; 14: 1285-1293.

32) Dai J, Ma J, Yu B, Zhu Z, Hu Y. Long noncoding RNA TUNAR represses growth, migration, and invasion of human glioma cells through regulating miR-200a and Rac1. Oncol Res 2018; 27: 107-115.

33) Hu GD, Wang CX, Wang HY, Wang YQ, Hu S, Cao ZW, Min B, Li L, Tian XF, Hu HB. Long noncoding RNA CCAT2 functions as a competitive endogenous RNA to regulate FOXC1 expression by sponging miR-23b-5p in lung adenocarcinoma. J Cell Biochem. 2018 Dec 12. doi: 10.1002/jcb.28077. [Epub ahead of print]

34) Mokhlis HA, Bayraktar R, Kabil NN, Caner A, Kahraman N, Rodriguez-Aguayo C, Zambalde EP, Sheng J, Karagoz K, Kanlikilicer P, Abdel Aziz AAH, Abdelghany TM, Ashour AA, Wong S, Gatza ML, Calin GA, Lopez-Berestein G, Ozpolat B. The modulatory role of microRNA-873 in the progression of KRAS-driven cancers. Mol Ther Nucleic Acids 2019; 14: 301-317.

35) Gong H, Fang L, Li Y, Du J, Zhou B, Wang X, Zhou H, Gao L, Wang K, Zhang J. MiR873 inhibits colorectal cancer cell proliferation by targeting TRAF5 and TAB1. Oncol Rep 2018; 39: 1090-1098.

36) Karabulut M, Alis H, Bas K, Karabulut S, Afsar CU, Oguz H, Gunaldi M, Akarsu C, Kones O, Aykan NF. Clinical significance of serum claudin-1 and claudin-7 levels in patients with colorectal cancer. Mol Clin Oncol 2015; 3: 1255-1267.

37) Hahn-Stromberg V, Askari S, Befekadu R, Matthiessen P, Karlsson S, Nilsson TK. Polymorphisms in the CLDN1 and CLDN7 genes are related to differentiation and tumor stage in colon carcinoma. APMIS 2014; 122: 636-642.